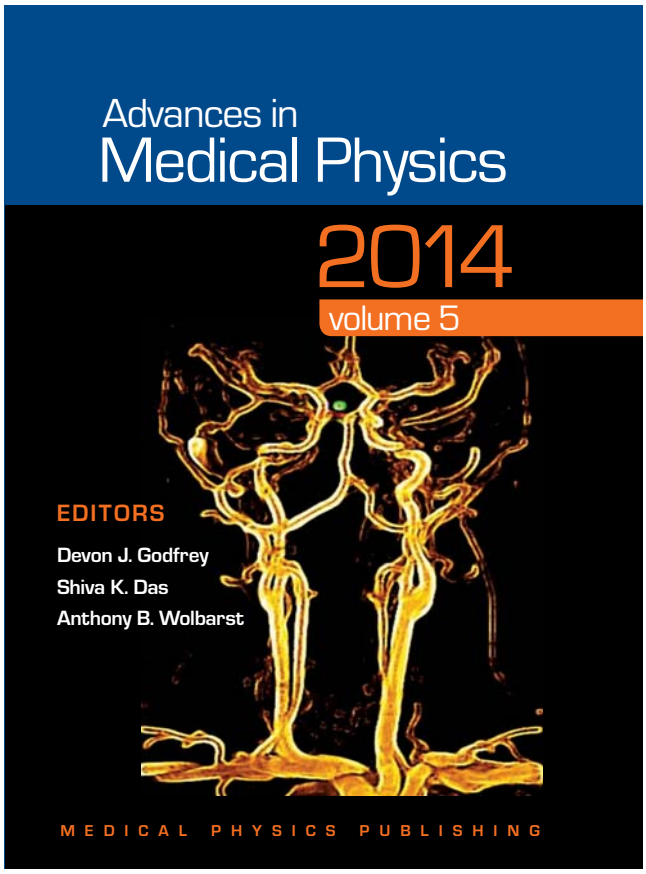


**Here is a sample chapter from this book.**

# Advances in Medical Physics 2014

Volume 5

# Advances in Medical Physics 2014 Volume 5

Edited by

Devon J. Godfrey
Duke University

Shiva K. Das
Duke University

Anthony B. Wolbarst
University of Kentucky

MEDICAL PHYSICS PUBLISHING
Madison, Wisconsin

Back cover images are from *Quantitative MRI in Cancer* and are reprinted courtesy of Taylor and Francis, New York. The front cover image is adapted from the same book.



20 19 18 17 16 15 14 1 2 3 4 5 6

Advances in Medical Physics series ISSN: 2156-2008

*Advances in Medical Physics–2014, Volume 5*

Volume 5 hard cover:
ISBN: 978-1-930524-63-7

Volume 5 eBook:
ISBN: 978-1-930524-72-9

Medical Physics Publishing
4513 Vernon Boulevard
Madison, WI 53705-4964
Phone: 800-442-5778
Fax: 608-265-2121
www.medicalphysics.org

Printed in the United States of America

# Dedication

Volume 5 of *Advances in Medical Physics* is dedicated
with great appreciation and affection

to Bill Hendee

in celebration of his retirement.
Bill is a wonderful friend to all of us who have had
the exceptional good fortune to know him.

*"If your actions inspire others to dream more, learn more,
do more and become more, you are a leader."*
–John Quincy Adams

# Contents

# Volume 5

# Preface

This is the fifth volume in the biennial series *Advances in Medical Physics*, designed to help medical physicists, technically inclined physicians, and other professionals stay current in medical radiation science and technology—and in particular, in sub-fields of medical physics other than their own.

Volume 5 contains an expanded focus on radiation oncology topics, including the new GammaPod $^{60}$Co device for breast radiosurgery, the allure of targeted dose enhancement via gold nanoparticles, strategies and devices for respiratory motion management, proton therapy fundamentals, and novel high-resolution 3D dosimeters that can be employed for the precise dose verification of complex treatment plans.

Radiation protection subjects include the role of the ICRP and IAEA in medicine and a comprehensive review of the many types of dosimeters available for monitoring personnel exposure.

Finally, the field of imaging is well represented, as always, with fascinating chapters highlighting novel x-ray photonics and phase contrast imaging technologies, state-of-the-art PET and cardiac SPECT implementations, the fundamentals of parallel MRI, advanced MRI sequences, and the first part of a suggested road map for teaching MRI to engineering and medical physics students.

The editors of *AMP–2014*
Devon Godfrey, Shiva Das, and Anthony Wolbarst
July 2014

# Contributors

**Bijan Arjomandy**
Senior Proton Medical Physicist
McLaren Proton Therapy Center
Flint, MI
bijan.arjomandy@mclaren.org

**Ross Berbeco**
Associate Professor
Department of Radiation Oncology
Brigham and Women's Hospital
Dana-Farber Cancer Institute
Harvard Medical School
Boston, MA
rberbeco@lroc.harvard.edu

**Thomas Beyer**
Professor and Deputy Director
Center for Medical Physics and Biomedical Engineering
Medical University of Vienna
Vienna, Austria
thomas.beyer@meduniwien.ac.at

**Claire Cousins**
Chair
International Commission on Radiological Protection (ICRP)
Consultant Interventional Radiologist
Addenbrooke's Hospital
Cambridge, UK
claire.cousins@addenbrookes.nhs.uk

**Shiva Das**
Professor
Department of Radiation Oncology
Duke University Medical Center
Durham, NC
shiva.das@duke.edu

**Peter Edic**
Principal Engineer
CT, X-ray and Functional Imaging Laboratories
GE Global Research
Niskayuna, NY
edic@ge.com

**Steven Feigenberg**
School of Medicine
University of Maryland
Baltimore, MD
sfeigenberg@umm.edu

**Devon J Godfrey**
Assistant Professor
Department of Radiation Oncology
Duke University Medical Center
Durham, NC
devon.godfrey@duke.edu

**Steven J. Goetsch**
Senior Medical Physicist
Dade Moeller Health Group
Solana Beach, CA
stevegoetsch@sdgkc.com

**Kevin F. King**
Senior Scientist
GE Healthcare
Waukesha, WI
kevin.f.king@med.ge.com

**Susanne M. Lee**
Senior X-ray Detector Engineer
Radiography Inspection Technologies
General Electric Measurement and Control
Troy, NY
lees@ge.com

**Hong Liu**
Professor and Smith Chair in Biomedical Engineering
School of Electrical and Computer Engineering
University of Oklahoma
Norman, OK
liu@ou.edu

**Daniel A. Low**
Professor and Vice Chair of Medical Physics
Department of Radiation Oncology
University of California
Los Angeles, CA
dlow@mednet.ucla.edu

**Mark T. Madsen**
Professor
Department of Radiology
University of Iowa College of Medicine
Iowa City, IA
mark-madsen@uiowa.edu

**Sudeep Mandal**
Photonic Device Scientist
Photonics Laboratory
Micro and Nano Structures Technologies
GE Global Research
Niskayuna, NY
sudeep.mandal@ge.com

**Osama Mawlawi**
Professor
Section Chief of Nuclear Medicine Physics
Department of Imaging Physics
MD Anderson Cancer Center
Houston, TX
omawlawi@mdanderson.org

**Ahmed Meghzifene**
Dosimetry and Medical Radiation Physics Section Head
Division of Human Health
Department of Nuclear Sciences and Applications
International Atomic Energy Agency (IAEA)
Vienna, Austria
a.meghzifene@iaea.org

**Fanbo Meng**
System Architect
GE Healthcare China
fanbo.meng@ge.com

**Yildirim D. Mutaf**
School of Medicine
University of Maryland
Baltimore, MD
ymutaf@umm.edu

**Elizabeth Nichols**
School of Medicine
University of Maryland
Baltimore, MD
enichols1@umm.edu

**Mark Oldham**
Professor
Department of Radiation Oncology
Duke University Medical Center
Durham, NC
mark.oldham@duke.edu

**Ronald R. Price**
Professor
Department of Radiology
Vanderbilt University Medical Center
Nashville, TN
ron.price@vanderbilt.edu

**John Rong**
Associate Professor
Department of Imaging Physics
The University of Texas MD Anderson Cancer Center
john.rong@mdanderson.org

**Brian Scherer**
Processing Engineer
Thin Films Laboratory
Micro and Nano Structures Technologies
GE Global Research
Niskayuna, NY
brian.scherer@ge.com

**Charles Smith**
Professor of Neurology & Radiology
University of Kentucky College of Medicine
Director, UK Magnetic Resonance Imaging and Spectroscopy Center
Lexington, KY
csmith@mri.uky.edu

**David H. Thomas**
Department of Radiation Oncology
University of California
Los Angeles, CA
dhthomas@mednet.ucla.edu

**Jacob Van Dyk**
Professor Emeritus
Departments of Oncology and Medical Biophysics
Western University
London, Ontario, Canada
vandyk@uwo.ca

**Anthony B. Wolbarst**
Associate Professor of Medical Physics Emeritus
University of Kentucky College of Medicine
Lexington, KY
awolbarst2@outlook.com

**Xizeng Wu**
Professor
Department of Radiology
University of Alabama at Birmingham
School of Medicine
xwu@uabmc.edu

**Nathan E. Yanasak**
Assistant Professor, Georgia Regents University
Director, Core Imaging Facilities for Small Animals
Augusta, GA
nyanasak@gru.edu

**Cedric Yu**
School of Medicine, University of Maryland
Baltimore, MD
Xcision Medical Systems
Columbia, MD
cyu002@umaryland.edu

**Da Zhang**
Medical Physicist
Department of Radiology
Massachusetts General Hospital
zhang.da@mgh.harvard.edu

# Contents of Previous Volumes of Advances in Medical Physics

## Volume 1–2006



## Volume 2–2008

## Volume 3–2010

## Volume 4–2012

---

* Corresponding author
† Reprinted originally as "An Approach to Assessing Stochastic Radiogenic Risk in Medical Imaging." *Med. Phys.* 38(12):1–5, 2015. Reprinted with permission from the American Association of Physicists in Medicine (AAPM).

# Passive Dosimeters for Personnel and Patient Dosimetry

*Steven J. Goetsch, Ph.D.*
*Senior Medical Physicist*
*Dade Moeller Health Group*
*Solana Beach, CA*

## 6.1 Introduction

### 6.1.1 Physical Principles

A dosimeter is a device that responds to ionizing radiation in some predictable manner. Attix gives this definition in his textbook on radiological physics: "A dosimeter can be defined generally as any device that is capable of providing a reading $r$ that is a measure of the absorbed dose $D_g$ deposited in its *sensitive volume V* by ionizing radiation." (Attix 1986). *Passive dosimeters* are often thought of as being synonymous with "personnel dosimeters," but more properly, passive dosimeters are those which "store" a reading in some latent form for later analysis. *Active dosimeters*, by contrast (e.g., cable-connected ionization chambers or diodes connected to an electrometer) give immediate visual readout of a signal, which may then require some analysis to be converted to absorbed dose. This chapter will consider recent developments in passive dosimeters, including some which have been in use for many years.

Dosimeters are a category of transducers that convert the energy latent in ionizing radiation into some quantifiable form that can be accurately converted into some measure of absorbed dose (or dose equivalent for personnel dosimeters). It is important to note that the "dose to dosimeters" is essentially irrelevant, except for degradable dosimeters such as diodes, which suffer damage with exposure to high levels of radiation. Dosimeters are, in fact, a proxy for personnel or the environment which is to be protected from the effects of ionizing radiation. No dosimeter is capable of exactly mimicking the response of human beings or animal species, but still it may provide useful estimates of the unknowable effects of absorbed radiation dose on a human being or object of interest. Many dosimeters claim to be "tissue equivalent," which usually means that their mean atomic number is similar to that of the standard four-element International Commission on Radiation Units and Measurement (ICRU) model for tissue. The ICRU specifies for a 30 cm tissue equivalent sphere a mass composition of 10.1% hydrogen, 11.1% carbon, 2.6% nitrogen, and 76.1% oxygen, with a density of 1 g/cm$^3$ (ICRU 1993). The classic A-150 tissue equivalent plastic is formulated from polyethylene and Zytel nylon with 16% carbon black and 3.6% calcium fluoride added (Smathers 1977).

### 6.1.2 Personnel Dosimetry Standards

Measurements of ionizing radiation from the earliest days of the work of Roentgen, Becquerel, and the Curies took two general forms: active dosimeters, such as Pierre Curie's gold leaf electroscope, and passive dosimeters, such as human skin reddening (erythema) and darkening of photographic film. This led to the development of two kinds of dosimetry standards. Personnel monitoring by means of carrying a photographic plate to assess cumulative exposure was suggested at a 1907 meeting of the American Roentgen Ray Society (Brodsky 1995). Secondly, "skin erythema dose" was described as early as 1923 and was still discussed in scientific literature as late as 1952 (Mutscheller 1928). Mutscheller recommended limiting the exposure of x-ray workers to 0.01 of the skin erythema dose in a 30-day period, later estimated to correspond to an annual dose of about 72 rads! The Roentgen was defined in 1928 by the Second International Congress of Radiology in Stockholm as "the quantity of radiation which liberates by ionization one esu of electricity per cm$^3$ of air under normal conditions of temperature and pressure" (Bushong 1995). This operational definition gave rise to dosimeters, such as the Victoreen condenser R meter which stored ionization in the form of discharged capacitors and was read out directly in Roentgens from a specialized reader/charging station.

## 6.2 Radiochromic Film

### 6.2.1 Original Purpose and Physical Mechanism

Direct color-changing (radiochromic) films which respond to ionizing radiation were first introduced in about 1970 for very high absorbed doses ($10^4$ to $10^6$ Gray) for monitoring sterilization of food products, medical supplies, and other things. International Specialty Products (now Ashland, Inc.) introduced the first self-developing radiochromic film for radiographic purposes as Gafchromic DL-1260 (later renamed HD-810) in 1986. This film could be used in the range of 25 to 2500 Gy (double-sided emulsion), and single-sided MD-55 film was available for doses ranging from 10 to 100 Gy. American Association of Physicists in Medicine (AAPM) *Report 63* of Task Group 55 described the nature of the radiochromic process and made recommendations for its clinical uses, including the subtleties of the readout process (Niroomand-Rad 1998). That reference states "Radiochromic dosimeters color directly and do not require chemical processing—a color change (colorless to blue, red, green, etc.) indicates exposure to radiation. Image formation occurs as a dye-forming or a polymerization process, in which energy is transferred from an energetic photon or particle to the receptive part of the leuko-dye or colorless photomonomer molecule, initiating color formation through chemical changes." McLaughlin and others at the National Institute of Standards and Technology (NIST) investigated the dosimetric properties of radiochromic media in photon and electron radiation therapy (McLaughlin 1988). A modern film consists of a thin active layer of microcrystalline monomeric polydiacetylene dispersion coated on a polyester film base (McLaughlin 1991). Readout of these films requires either a densitometer or spectrophotometer (Klassen 1997). These authors used a spectrophotometer with a wavelength of 676 nm (deep red) and a bandpass of 3.5 nm. Care must be taken with some double emulsion films, as the polarized light from the readout

device may produce different results if the film is rotated 90 degrees before scanning. In recent years, more sophisticated spectral analysis techniques divided the film coloration up into two or three color bands.

### 6.2.2 Introduction to Radiology and New Films

Products were introduced later with increased sensitivities, such as HS for high-energy photon beams above 1 MeV and XR-T for low-energy photon beams below 0.1 MeV (Devic 2004). Investigators with access to high-quality spectral microdensitometers were able to separately measure the transmittance of the radiochromic film (RCF) in two different spectral peaks, one at about 610 nm and the other at about 672 nm, to extend the dynamic range of the system (Lee 2005). A new model designated as EBT radiochromic film was introduced in 2005 with improved flatness and symmetry, which had been somewhat problematic in earlier films. The film was immediately applied to intensity-modulated radiation therapy (IMRT) patient QA measurements. A newer version called EBT2 (Figure 6–1a) was introduced in 2009 which added a yellow dye (Lindsay 2010), that successfully decreased the sensitivity of the film to visible light, although the active component of the film was unchanged. The authors noted that the energy response of the film drifted over time from batch to batch and tended to under-respond up to 20% at 105 kVp due to variation in the amount of chlorine incorporated in the film. Another group of authors found lower energy dependence with the new EBT2 film in the high-energy range (flat within ±0.6% from 100 keV to 18 MeV (Sutherland 2010). However, they found an energy response that varies by 10% to 50% at low photon energies, depending on the batch. Another study showed inhomogeneity within the same piece of film causing dose uncertainties across the film of nearly 9% at 1 Gy (Hartmann 2010). EBT2 film has a single active layer 30 μm in thickness, while the older EBT formulation had two layers 17 μm in thickness sandwiching a "surface" layer. The substrate layers were also increased to 225 μm in total thickness (thicker on the bottom) versus 194 μm in thickness (two equally thick layers) in the original film. The introduction of this new EBT2 film was quite successful, and it was cited in dozens of medical physics abstracts in the first two years after its launch for a wide variety of applications, including stereotactic radiosurgery small field dosimetry, HDR applications, and proton beam dosimetry. Another new product is EBT3 film designed for use with low-energy diagnostic x-ray machines and CT scanners (Figure 6–1b). It has a dose range of 1 cGy to 40 Gy with an active layer 30 μm thick. It is designed for red light measurements with a peak at 630 nm.

### 6.2.3 Radiological Applications

Within the last two years, three new radiochromic film types have been introduced: Gafchromic HD-V2 is designed for the quantitative measurement of high-energy photons, protons, and electrons in the range of 10 to 1000 Gy with an active layer only 8 μm thick. The new type MD-V3 film, with an active layer 15 μm thick, is designed for use with high-energy photons in the dose range of 1 to 100 Gy. It is a replacement for MD-V2-55. A special film called RTQA2 was developed for quality assurance in radiation therapy, such as radiation field/light field alignment measurements, star shots, and brachytherapy QA films (Figure 6–1c). It has a dynamic range from 0.02 to 8 Gy with an active layer 17 μm thick and a quoted spatial resolution of 5000 dpi.

The use of EBT2 film has been reported for such diverse applications as synchrotron radiation (Brown 2012), mailed dosimetry for Radiation Therapy Oncology Group (RTOG) lung protocols (Kry 2013), and dose re-optimization in radia-

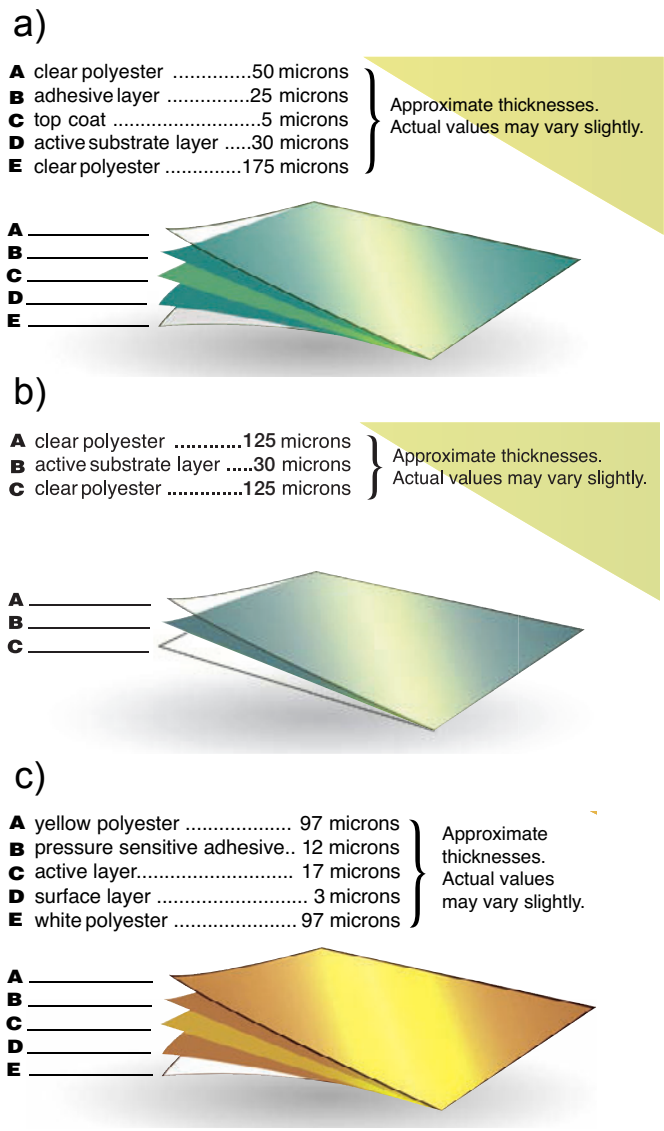


Figure 6–1. Dosimetry films. a) Five-layer EBT2 and b) three-layer EBT3 laminated films. c) Configuration and structure of five-layer laminated Gafchromic RTQA2 film. It is made by laminating an active layer between two polyester layers, which allows water immersion. (Courtesy of Ashland, Inc.)

tion therapy to take account of the cumulative dose from cone-beam CT scans during treatment (Akino 2012). Another manuscript compared two arc-therapy plans, one with 6 MV x-rays using conventional dose delivery versus similar plans using 10 MV flattening filter-free x-rays (Ong 2012). Some authors have noted that modern flatbed scanners can spectroscopically analyze the radiochromic film in red, blue, and green channels, which may be interrogated separately to further analyze dose response (Micke 2011).

In conclusion, radiochromic films have earned an important place in passive dosimetry as the ascending standard in 2D dosimetry. With the demise of x-ray film processors, the self-developing nature of these films and their admirable dosimetric qualities and wide variety of film types assure their status as important assets in the arsenal of the modern 21st century radiological physicist.

## 6.3 Thermoluminescent Dosimeters (TLDs)

### 6.3.1 History of TLDs

The history of using thermoluminescence as a dosimeter goes back to the early 1950s when Professor Farrington Daniels of the University of Wisconsin consulted with the Atomic Energy Commission on dosimetry for open-air nuclear weapons testing. It was known that certain inorganic materials stored energy in electron traps which would later be given off, in the form of light, upon heating. The bequest of a single jar of lithium fluoride from Harshaw Chemical Company (Solon, OH) to newly arrived Professor of Physics and Radiology John Cameron led to the invention of TLD 100, TLD 600, and TLD 700, each named for the dominant lithium nuclide (Cameron 1961, 1964). TLD 100 uses natural lithium, with about 92.5% abundance of $^{7}$Li and 7.5% abundance of $^{6}$Li. Since $^{6}$Li readily absorbs neutrons (making it a valuable material for nuclear weapons) TLD 600 (with enriched levels of $^{6}$Li) is sensitive to neutrons, while TLD 700 (with most of the $^{6}$Li removed) is relatively insensitive to neutrons but remains sensitive to photons. TLD 100 is sensitive to both neutrons and photons. Each of these formulations relies on doping with parts per million of magnesium and titanium. Serendipitously, a replacement for the original jar of lithium fluoride, produced very poor TLD dosimeters. When samples from both jars were sent to Argonne National Laboratories for atomic analysis, the first jar was reported to have Mg and Ti in very low levels. This later turned out to be a lab error, but doping of the second, much purer batch of lithium fluoride with these impurities led to the patented TLD series of dosimeters. Another important material for TLD is $CaF_2$ crystals which, although more sensitive to radiation, have the disadvantage of being sensitive to visible light.

Historically, TLD dosimetry has been extremely important in radiological dosimetry, especially in terms of quality assurance and patient dosimetry. Gentry and DeWerd reviewed the 20-year history (now approaching 35 years) of the University of Wisconsin–Madison's Radiation Monitoring by Mail service, specializing in skin entrance exposure (later mean glandular dose) for patients undergoing mammography (Gentry 1996). This service was the first in the United States to allow remote institutions to receive TLD dosimeters by mail, place them on the skin of patients undergoing mammographic examinations, and then receive a readout from a reputable university scientific laboratory. Results of over 4400 mammograms at over 170 centers had been measured and reported by the time of that report. This service became a semi-official recommended screening service for the American Cancer Society and led to the development of the American College of Radiology mammography quality assurance program. Around the same time, in 1977, the Radiological Physics Center (RPC) at the M.D. Anderson Medical Center in Houston, TX, implemented a mailed dosimetry system for high-energy photons and electrons in radiation therapy centers across the United States (Kirby 1986). These authors reported that the system allowed local institutional standards to be compared to a national standard with an accuracy of about 1% (nearly 2500 reported measurements with an overall average of mailed results to local standards of 0.999 for photons and 1.020 for electrons). Sometimes problems at the 5% or higher level were detected, including one very unfortunate series in a high-altitude center where a miscalibrated barometer led to the overdosing of many patients. Years of on-site visits by RPC physicists and annual TLD mailed dosimetry led to a significantly tighter agreement nationwide on the value of absorbed dose, leading to the role of the RPC as gatekeeper for Radiation Therapy Oncology Group (RTOG) national radiation therapy protocols.

There has been very little progress in the field of thermoluminescent dosimetry for many years in terms of new phosphors or new readout methods. A number of phosphors (TLD-300 based on calcium fluoride doped with thulium; TLD-800 lithium borate doped with manganese; TLD-900 calcium sulphate doped with dysprosium; magnesium silicate doped with terbium) have been introduced and found niche uses. However, the original family of TLD dosimeters have proved remarkably adept at providing useful information in the most advanced radiation therapy techniques of the early 21st century.

### 6.3.2 Physical Processes

Thermoluminescence occurs in many materials, thousands of which occur naturally, making them extraordinarily useful in archeological dating of pottery and bone fragments. A crystal such as LiF or $CaF_2$ can be doped with parts per million of an impurity, such as magnesium or titanium, to produce trapping centers and luminescence centers. These centers provide metastable states several electron volts above ground level.

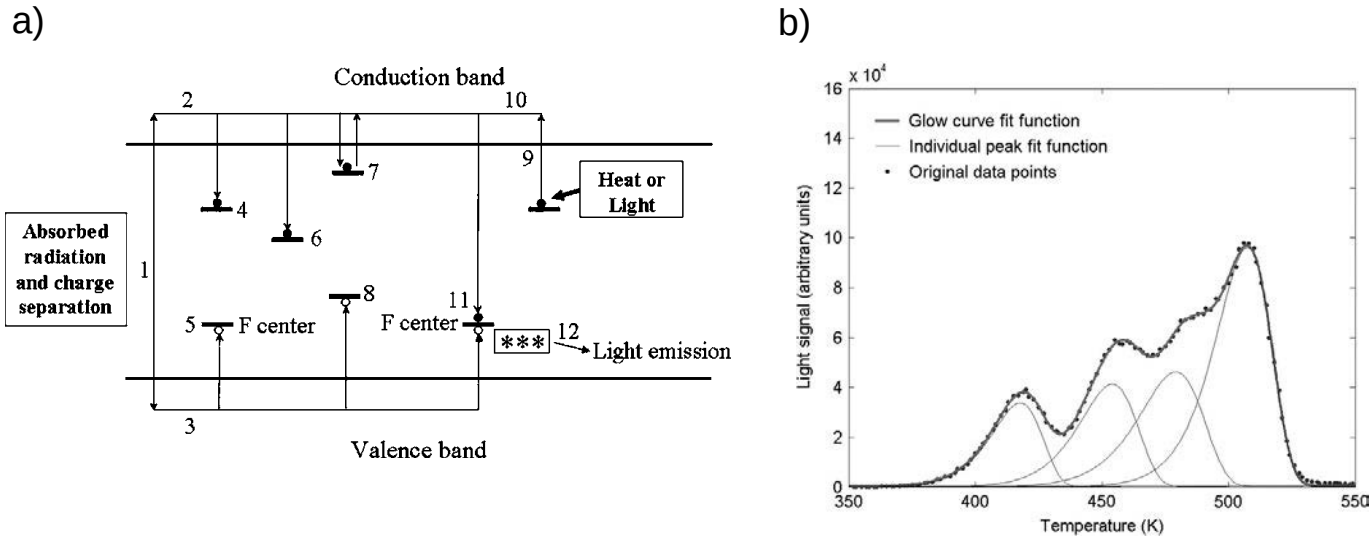


Figure 6–2. Thermo- and optical luminescence. a) The energy levels of a crystalline material that sustains thermoluminescence or optical luminescence: (1) absorption of radiation and subsequent charge separation; (2) migration and trapping of an electron, ●, and (3) hole, ○, after charge separation; (4) Moderately deep electron and (5) hole traps; (6) very deep and (7) shallow electron traps; (8) ejection of electron from trap with absorption of heat (thermoluminescence), or light (optical luminescence); (9) migration of untrapped electron; (10) recombination of electron and hole at hole trap; (11) emission of light at luminescence center, ***, which received energy from the electron-hole recombination. OSLD conduction electrons (from Jursinic 2007). b) TLD glow curve (from Harvey 2011).

An electron may be promoted to these levels by absorbing energy from ionizing radiation and remain trapped in these states. Some of these electrons fall down to the ground state due to random thermal energy, while others remain trapped there until deliberately released in a specially designed heater or laser readout device (Figure 6–2a). Typically, samples are stored for 24 hours to let natural fading take place. Subsequently, TLDs suffer from fading over a period of days or months. This process is irreversible—the TLD dosimeter can only be read out one time. Heating up a TL material at a fixed rate produces a "glow curve" which can be integrated by a photometer. TLD-100 has five well-characterized peaks (Harvey 2011) (Figure 6–2b).

### 6.3.3 Clinical Applications

One group of researchers in Switzerland used TLD 100 (Thermo Fisher Scientific, Waltham, MA) in an Alderson RANDO phantom (Radiology Support Devices, Long Beach, CA) to measure scattered dose outside the target of radiation therapy volumes with seven different linear accelerator systems (Hälg 2012). The authors were able to reach a number of useful conclusions:

- flattening filter-free irradiation techniques showed the least amount of stray dose;
- IMRT techniques resulted in stray doses which scaled well with the total monitor units applied;
- the use of hard wedges instead of dynamic wedges caused a significant increase in stray dose, and
- stray dose was higher for the Accuray Cyberknife than for the Accuray Tomotherapy or other rotational linacs.

Other investigators in London used TLDs to measure skin dose for patients undergoing radiation therapy with a 50 kV dedicated x-ray breast intraoperative irradiation device (TARGIT trial) (Eaton 2011). A team from the University of California–Davis assessed skin dose effects from the use of a brass mesh for chest wall irradiation patients (instead of the normal tissue-equivalent bolus) using TLD dosimeters for all 16 patients. Four had both TLD and MOSFET dosimeters, which agreed reasonably well with each other (Healy 2012).

Another group from Sydney, Australia, studied the dose enhancement from repeated use of megavoltage cone-beam CT to position patients for radiation therapy of the breast (Quinn 2012). They found that a weekly MV CBCT scan contributed 0.5% and 17%, respectively, to the total ipsilateral and contralateral breast dose, which could lead to a statistically noticeable increase in a radiation-induced second tumor.

## 6.4 Optically Stimulated Luminescence Dosimeters (OSLD) and Radiophotoluminescent Dosimeters (RPL)

### 6.4.1 Physical Processes of OSLD and Similarity to TLD

Optically stimulated luminescence is a process that has been known since at least 1985 when it was applied to quartz

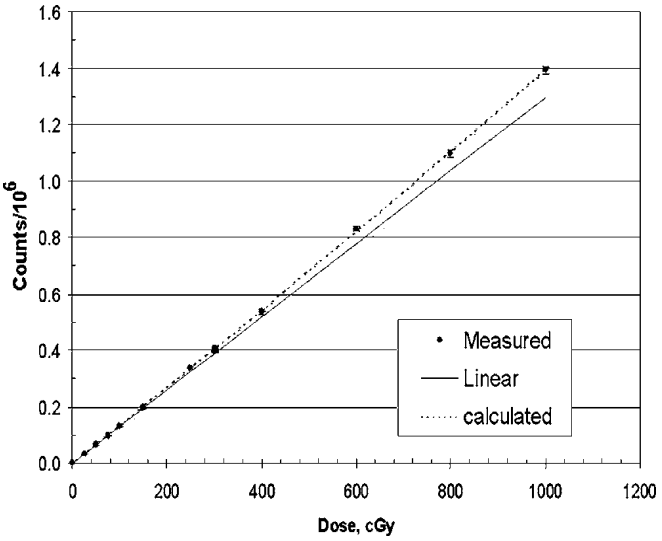


Figure 6–3. OSLD response vs. absorbed dose from 6 MV x-rays (from Jursinic 2007).

archeological samples before it was applied to radiation dosimetry beginning about 1999 (Jursinic 2007). The optically stimulated luminescence phenomena closely resembles thermoluminescence, with the important difference that OSL dosimeters can be stimulated by light and read out repeatedly, even during the irradiation process, making them near real-time dosimeters. This was actually a serendipitous discovery when early samples of aluminum oxide were prepared as TLDs and suffered seriously from accidental bleaching of signal by visible light. The recombination centers in aluminum oxide are created primarily by oxygen vacancies and are called F centers, between the valence and conduction band. TL and OSL are therefore competing effects in the same material. Some low-energy electron traps can be triggered (with resulting light emission) by ambient room temperatures, while others are triggered in the heated pan of a TL reader. The OSL effect was used to create OSLDs which have a peak of effective stimulation at wavelength of about 475 nm. These dosimeters can be read out in either the continuous wave (CW) mode or in pulsed mode.

Natural samples exhibiting OSLD properties have been replaced by aluminum oxide samples doped with carbon ($Al_2O_3$:C), the same chemical formula as ruby and sapphire in its pure form. OSLD dosimeters are now available from Landauer, Inc. (Glenwood, IL) as their nanoDot™ dosimeters and microStar® readers. The dosimeters contain OSLD material inside a lightproof plastic holder and are a few millimeters thick and 10 mm x 10 mm square. Landauer supplies both National Voluntary Laboratory Accreditation Program (NAVLAP) certified personnel dosimeters (Luxel™ and InLight™) as well as loose dosimeters for on-patient dosimetry. They have a stated energy range from 5 keV to 20 MeV and a lower limit of detection of 0.1 mGray, with a nearly isotropic energy response and very linear dose response (Figure 6–3). The dosimeters are not, however, very tissue equivalent.

The Risø National Laboratory (Roskilde, Denmark) has manufactured OSLDs small enough to fit inside a brachytherapy HDR catheter. These OSLDs can be coupled with a fiber optic

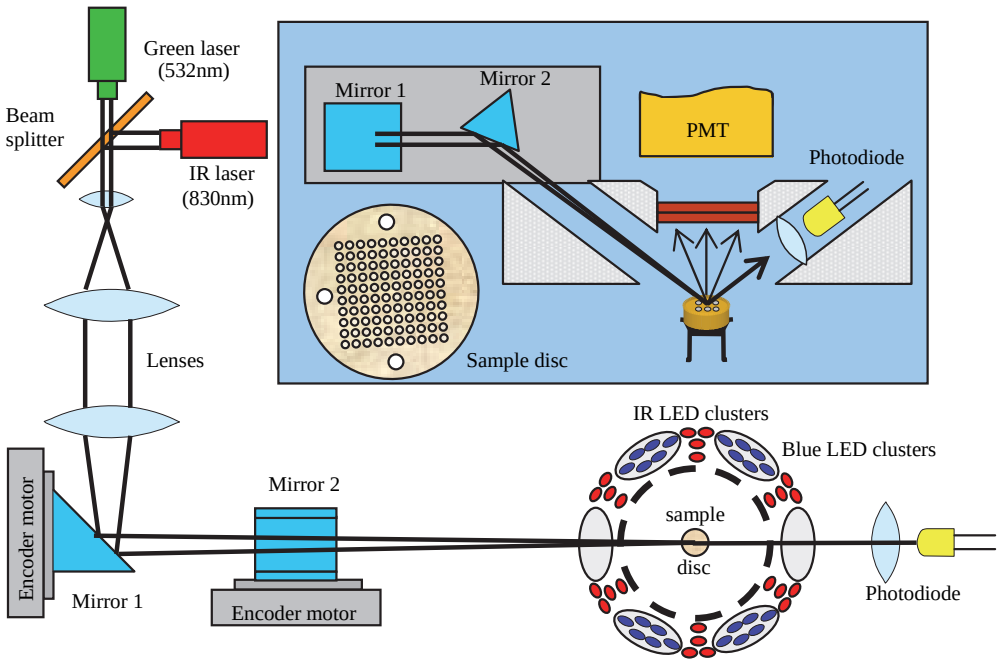


Figure 6–4. Risø National Laboratory Model TL/OSL-DA-20 reader (from Thomsen, 2004).

cable and the Model TL/OSL-DA-20 reader to give real- time readout during patient treatment (Aznar 2004) (Figure 6–4).

### 6.4.2 Radiological Applications of OSLD

One of the most interesting applications of the OSLD phenomena is a study utilizing ordinary table salt (NaCl) as an OSLD dosimeter in a contaminated village near Chernobyl, Belarus (Bernhardsson 2012). Readings taken in a depopulated area contaminated with cesium-137 were obtained from TLD material, an airborne radioactivity detector, and grocery store table salt read from the commercial reader. All three methods were in relatively good agreement.

A recent clinical paper from Rhode Island Hospital sought to analyze the real-time dosimetry applications of OSLD in high dose-rate remote afterloading brachytherapy, moving OSLD from the passive to the active category (Tien 2012). The authors concluded that the commercial system they tested was a low-cost, reusable, very accurate system for on-patient dosimetry. Another group studied OSLDs vs. EBT2 radiochromic film and ionization chamber for use in a basic physics measurement, assessing the backscatter factor for low-energy (20 to 100 kVp) superficial x-rays (Mart 2012). All three methods gave comparable results.

Proton therapy dosimetry was also explored by the Radiological Physics Center in Houston, TX, for Bragg peak protons between 160 and 250 MeV using the nanoDot dosimeter from Landauer (Kerns 2012). With the growing popularity of proton beam radiation therapy and the highly individualized treatment plans for each patient, the necessity of finding a low-cost, reliable, and accurate dosimeter for individual patient treatment plans is very important. There is a small supralinearity from 200 cGy (1%) to 1000 cGy (5%), but it is reproducible and can be accounted for. There was little energy dependence, and in-phantom results agreed well with ionization chamber measurements. OSLD has become increasingly popular as a personnel dosimeter (Figure 6–5).

### 6.4.3 Radiophotoluminescent (RPL) Dosimetry

Radiophotoluminescent Dosimetry, closely related to OSLD and TLD, was first described in 1949 (Becker 1968) and has also been used in radiation oncology (Araki 2003, Perks 2005). Certain silver activated phosphate glass compounds form stable color centers (optically active point defects) when irradiated; these can then be stimulated by pulsed ultraviolet lasers to give off light (optical fluorescence) which can be measured and correlated with absorbed dose. The active volume of commercial glass rods (AGC Techno Glass, Shizuoka, Japan) is extremely small, measuring 1 mm in diameter by 0.6 mm in depth.

A group of Japanese clinicians used RPL glass rods to mount a large *in vivo* dosimetry study of interstitial brachytherapy patients (Nose 2008), assessing the accuracy of dosimetry calculations in 66 patients undergoing HDR treatment for pelvic malignancy, assessing a total of 1004 points. The mean agreement of measured to calculated dose was 0.98, giving high confidence to this irradiation technique and measurement device. Model GD-301 RPL glass rods were also irradiated in a 200 MeV proton beam at the National Cancer Center in Goyang, Korea, in a polymethylmethacrylate phantom (Rah 2012). The glass rods did an excellent job of duplicating the dose and crossbeam profile as measured by calibrated ionization chambers. The Center plans to employ these RPL dosimeters for *in vivo* dosimetry.


Figure 6–5. The Landauer Luxel™ and InLight™ personnel dosimeters.

## 6.5 Metal Oxide Semiconductor Field Effect Transistor (MOSFET) Dosimeters

### 6.5.1 Physical Processes

MOSFET dosimeters have been employed in specialized areas of radiation dosimetry since the 1980s (Hughes 1988, Gladstone 1991, Soubra 1994). The MOSFET is a unique electronic dosimeter, since it can be deployed as a separate unit, exposed to radiation, and then returned to a readout device, much as the classic Victoreen condenser "R" meter. The MOSFET is a sandwich device with a P-type semiconductor separated from a metal gate by an insulating oxide layer (Figure 6–6a). The gate voltage necessary to allow conduction through this device is known as the threshold voltage. Upon exposure to ionizing radiation electrons, hole pairs are formed in the oxide insulation layer. The threshold voltage shift is proportional to the radiation dose absorbed in the oxide layer. These devices were first used as dosimeters for manned NASA space flights in the 1980s. The devices were custom fabricated at several universities and hospitals and began to be commercially distributed by Sicel Technologies

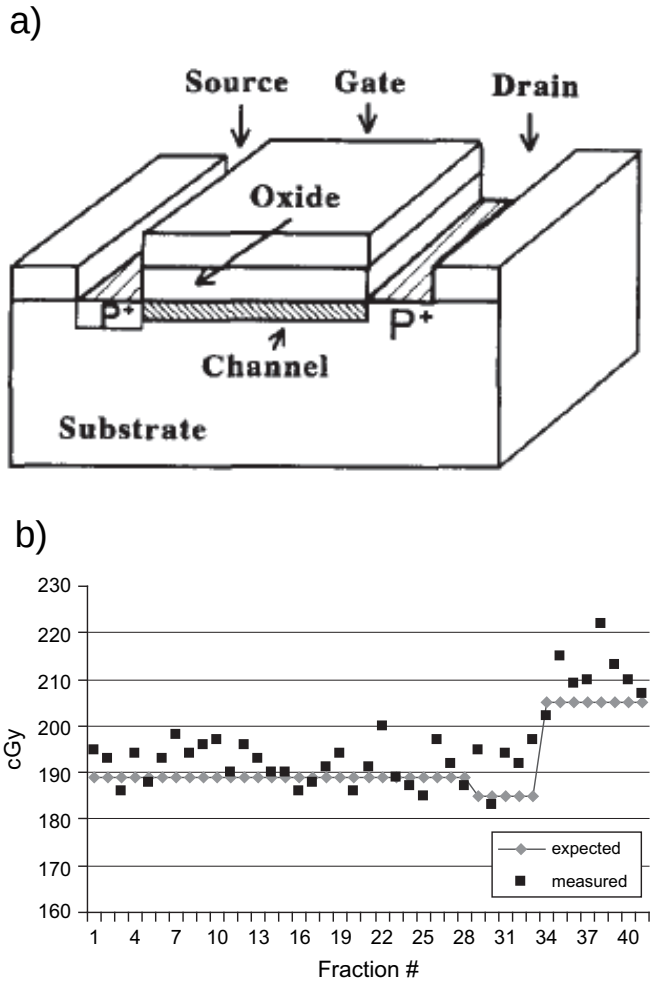


Figure 6–6. MOSFET Dosimetry. a) Diagram of a P channel MOSFET device, showing the oxide ($SiO_2$), the substrate (Si), the source, the gate, and the drain (from Soubra 1994). b) Pattern of daily dose measurements for an implanted MOSFET dosimeter comparing planned dose (gray diamonds) with measured dose (block squares) for a breast radiation therapy patient (from Scarantino 2008).

which, in 2002, added the remarkable innovation of wireless technology (radio-frequency identification, or RFID) to "broadcast" the dose from implanted dosimeters (Scarantino 2005). With the bankruptcy of Sicel Technologies in 2011, the OneDose dosimeters are no longer available.

Permanently implanted RFID MOSFET dosimeters were used to compare internally measured versus planned doses for 33 breast and 29 prostate patients (Scarantino 2008) (Figure 6–6b). Since the dosimeters were permanently placed and reusable, an average of 49 measurements were reported for each breast patient and 60 measurements for each prostate patient. This unique concept allowed the difference between planned and daily dose to be measured for each therapy fraction, as well as to assess migration of the implanted seeds themselves. Another study implanted a single RFID MOSFET dosimeter in each of 20 patients undergoing IMRT for prostate cancer (Den 2012). Measured doses were consistently >6% above predicted doses for 3 of the 20 patients. There were no significant deviations between planned doses and those from real-time cone-beam computed tomography (CBCT) obtained at the time of treatment delivery, but all three patients had new CT scans and were replanned accordingly. MOSFET measurements of the revised plans were all consistently within 6% of the planned doses. The authors recommended use of MOSFETs for extremely complex dose plans to assure accuracy of dose delivery. A similar report from a group of authors in Turkey used MOSFET dosimeters to verify field-in-field dosimetry for total body irradiation patients (Onal 2012). Another group at Indiana University reported MOSFET measurements for patients undergoing total body irradiation with a dedicated cobalt-60 device (Akino 2013). Feedback from fraction one allowed adjustments to be made in the final four fractions to achieve the goal of ±10% dose uniformity throughout the total body.

Japanese authors working at the National Cancer Center Hospital East proton therapy facility successfully compensated for the 26% under-response of a commercial MOSFET detector in the Bragg peak of a 190 MeV proton beam (Kohno 2011). They used the new dual temperature-compensated MOSFET TN-252RD detector (Best Medical, Ottawa) with two detectors fabricated on the same substrate with an active area of 0.2 x 0.2 $mm^2$. The MOSFET was compared in an anthropomorphic head phantom to measurements with a parallel plate ionization chamber. Results were good enough to encourage moving on to actual patient studies (Kohno 2012)

A novel experimental irradiation technique utilized the Cyberknife for experimental treatment in animals (dogs and pigs) for ablation of cardiac arrhythmias (Gardner 2012). Such cardiac disturbances, especially atrial fibrillation, affect 1 to 2% of the general U.S. population and are often treated with RF energy used to create a scar on the cardiac tissue. The radiation dose was delivered using the Synchrony mode of the Cyberknife to the beating hearts of living animals that had previously been implanted with both TLD-100 dosimeters and a catheter-placed MOSFET detector. Each dosimeter system gave dose estimates within 10% of the planned irradiation doses.

A final recent paper utilized MOSFETs in a unique study of quality control for high dose rate brachytherapy (Able 2013). The authors conducted a study on a gel prostate phantom with an iridium-192 HDR unit and 10 MOSFET dosimeters. An irradiation plan was developed for 12 needles and 129 dwell positions, which they delivered correctly 16 times, making measurements each time. Errors were then deliberately introduced into the plan (wrong patient, wrong calibration, incorrect needle placement, and others) prior to

irradiation, and statistical process control analysis was used to analyze the results. The authors concluded that this was a viable method for quality control for HDR procedures.

## 6.6 Alanine Dosimeters (EPR)

### 6.6.1 Physical Processes

Alanine is an α amino acid, chemical formula $CH_3CH(NH_2)COOH$, whose L isomer is one of 20 amino acids encoded by DNA. It is nearly tissue equivalent and has the property of trapping free radicals liberated by interaction with ionizing radiation (Wielopolski 1987). This dosimeter requires electron paramagnetic resonance (EPR) measurement in a specialized spectrometer in order to read out the absorbed dose. The EPR spectrum is the plot of the EPR signal from the unpaired electron as the spectrometer slowly increases the magnetic field, typically in the range of 0.335 tesla (3350 gauss) (Figure 6–7). Integration of this signal over a defined peak leads to the absorbed dose estimate. Alanine was originally incorporated into an agar gel to create a three-dimensional dosimeter, but most recently compact pellets of alanine as "point" dosimeters have become more popular (Far West Technologies, Goleta, CA).

Alanine pellets and thin films were assessed as dosimeters in the Ophthalmological Proton Therapy Installation in Switzerland at the Paul Scherer Institute using 62 MeV protons (Onori 1997). The dosimeters showed good agreement with ionization chamber measurements and excellent linearity of response with proton doses from 5 to 250 Gy. Alanine pellets were also used successfully to measure the 4 mm output factor of the Leksell Gamma Knife, one of the most challenging measurements in radiological physics (Mack 2002). Alanine also proved useful at the unique carbon ion facility at the Gesellschaft fur Schwerionenforschung (GSI) cyclotron in Darmstadt, Germany (Herrmann 2011). Researchers there irradiated alanine pellets (5.05 mm in diameter by either 2.27 or 0.44 mm thick) prepared by the British National Physical Laboratory (NPL) with seven monoenergetic carbon ion beams in the energy range of 89 to 400 Mev/u. The thick pellets were used in the 5 to 70 kGy range, while the thin pellets were used in the 40 to 70 kGy range. Good results were obtained after carefully determining energy calibration factors for these alanine dosimeters.

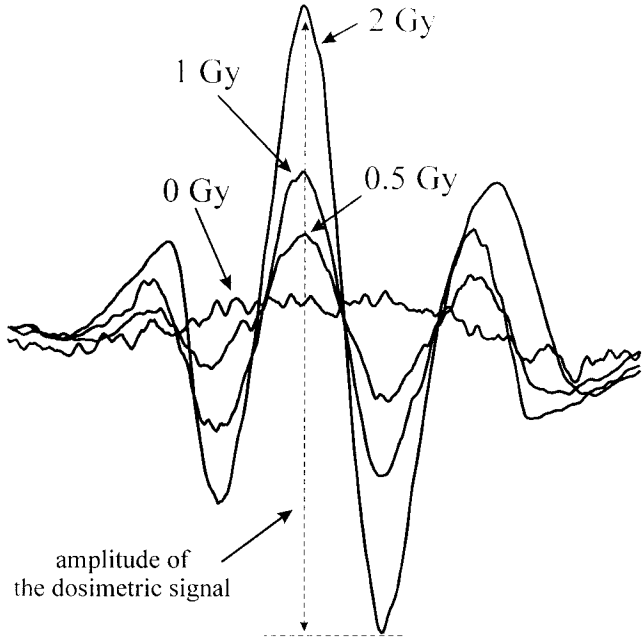


Figure 6–7. Typical EPR spectra of L-α-alanine after irradiation with single-fraction doses of 0.5, 1.0, and 2.0 Gy. The line marked 0 Gy is the background spectrum from a non-irradiated detector (from Cieselski 2003).

## 6.7 References

Able, C. M., M. Bright, and B. Frizzell. (2013). "Quality Control of High-Dose_Rate Brachytherapy: Treatment Delivery Analysis Using Statistical Process Control." *Int. J. Radiat. Oncol. Biol. Phys.* 85:828–833.

Akino, Y., M. Koizumi, I. Sumida, Y. Takahashi, T. Ogata, S. Ota, S. Isohashi, K. Konishi, and Y. Yoshioka. (2012). "Megavoltage Conebeam Tomography Computed Dose and the Necessity for Reoptimization for Imaging Dose-integrated Intensity-modulated Radiotherapy for Prostate Cancer." *Int. J. Rad. Oncol. Biol. Phys.* 82:1715–22.

Akino, Y., K. P. McMullen, and I. J. Das. (2013). "Patterns of Patient Specific Dosimetry in Total Body Irradiation." *Med. Phys.* 40:417 doi 10.1118/1.4795335.

Araki, F., T. Ikegami, T. Ishidoya, and H. Kubo. (2003). "Measurements of Gamma-Knife Helmet Output Factors Using a Radiophotoluminescent Glass Rod Dosimeter and a Diode Detector." *Med. Phys.* 30:1976–81.

Attix, F. H. *Introduction to Radiological Physics and Dosimetry.* New York: John Wiley & Sons, 1986.

Aznar, M. C., C. E. Anderson, L. Bøtter-Jensen, S. A. Bäck, S. Mattsson, F. Kjaer-Kristoffersen, and J. Medin. (2004). "Real-time Optical-fiber Luminescence Dosimetry for Radiotherapy: Physical Characteristics and Applications in Photon Beams." *Phys. Med. Biol.* 49:1655–69.

Becker, K. (1968). "Recent Progress in Radiophotoluminescent Dosimetry." *Health Phys.* 14:17–32.

Bernhardsson, C., S. Matskevich, S. Mattsson, and C. Rääf. (2012). "Comparative Measurements of the External Radiation Exposure in a 137Cs Contaminated Village in Belarus Based on Optically Stimulated Luminescence in NaCl and Thermoluminescence in LiF." *Health Physics* 103:740—749.

Brodsky, A., R. L. Kathren, and C. A. Willis. (1995). "History of the Medical Uses of Radiation: Regulatory and Voluntary Standards of Protection." *Health Phys.* 69:783–823.

Brown, T. A. D., K.R. Hogstrom, D. Alvarez, K. L. Matthews II, K. Ham, and J. P. Dugas. (2012). "Dose-response Curve of EBT, EBT2, and EBT3 Radiochromic Films to Synchrotron-produced Monochromatic X-ray Beams." *Med. Phys.* 39:7412–7417.

Bushong, S. (1995). "History of Standards, Certification and Licensure in Medical Health Physics." *Health Phys.* 69:824–36.

Cameron, J. R., F. Daniels, N. Johnson, and F. Daniels. (1961). "Radiation Dosimeter Utilizing the Thermoluminescence of Lithium Fluoride." *Science* 134:333–34.

Cameron, J. R., D. Zimmerman, G. Kenney, R. Buch, R. Bland, and R. Grant. (1964). "Thermoluminescent Radiation Dosimetry Utilizing LiF." *Health Phys.* 10:25–29.

Den, R. B., K. Nowak, I. Buzorovic, J. Cao, A. S. Harrison, Y. R. Lawrence, A. P. Dicker, and T. N. Showalter. (2012). "Implanted Dosimeters Identify Radiation Overdoses during IMRT for Prostate Cancer." *Int. J. Radiat. Oncol. Biol. Phys.* 83:e371–76.

Devic, S., J. Seuntjens, G. Hegyi, E. B. Podgorsak, C. G. Soares, A. S. Kirov, I. Ali, J. F. Williamson, and A. Elizondo. (2004). "Dosimetric Properties of Improved GafChromic Films for Several Digitizers." *Med. Phys.* 31:2392–401.

Devic, S., N. Tomic, S. Aldelaijan, F. DeBlois, J. Seuntjens, M. F. Chan, and D. Lewis. (2012). "Linearization of Dose-response Curve of the Radiochromic Film Dosimetry System." *Med. Phys.* 39:4850–57.

Eaton, D. J., B. Best, C. Brew-Graves, S. Duck, T. Ghaus, R. Gonzalez, K. Pigott, C. Reynolds, N. R. Williams, and M. R. S. Keshtgar. (2011). "*In Vivo* Dosimetry for Single-fraction Targeted Intraoperative Radiotherapy (TARGIT) for Breast Cancer." *Int. J. Rad. Oncol. Biol. Phys.* 892: e819–24.

Gardner, E. A., T. S. Sumanaweera, O. Blanck, A. K. Iwamura, J. P. Steel, S. Dieterich, and P. Maguire. (2012). "*In Vivo* Dose Measurement Using TLDs and MOSFET Dosimeters for Cardiac Radiosurgery." *J. Appl. Clin. Med. Phys.* 13:3745.

Gentry, J. R. and L. A. DeWerd. (1996). "TLD Measurements of *In Vivo* Mammographic Exposures and the Calculated Mean Glandular Dose Across the United States." *Med. Phys.* 23:899–903.

Gladstone, D. J. and L. M. Chin. (1991). "Automated Data Collection and Analysis System for MOSFET Radiation Detectors." *Med. Phys.* 18:542–48.

Hälg, R. A. and J. Besserer. (2012). "Systematic Measurements of Whole-body Dose Distributions for Various Treatment Machines and Delivery Technique in Radiation Therapy." *Med. Phys.* 39:7662–76.

Hartmann, B., M. Martisiková, and O. Jäkel. (2010). "Homogeneity of Gafchromic EBT2 Film." *Med. Phys.* 37:1753–56.

Harvey, J. A., M. L. Rodrigues, and K. J. Kearfott. (2011). "A Computerized Glow Curve Analysis (GCA) Method for WinREMS Thermoluminescent Data Using MATLAB." *Appl. Radiat. Isot.* 69:1282–86.

Healy, E., S. Anderson, J. Cui, L. Beckett, A. M. Chen., J. Perks, R. Stern, and J. Mayadev. (2013). "Skin Dose Effects of Postmastectomy Chest Wall Radiation Therapy Using Brass Mesh as an Alternative to Tissue Equivalent Bolus." *Practical Rad. Oncol.* 3:e45– e53.

Herrmann, R., O. Jäkel, H. Palmans, P. Sharpe, and N. Bassler. (2012). "Dose Response of Alanine Detectors Irradiated with Carbon Ion Beams." *Med. Phys.* 38:1859–66.

Hughes, R. C., D. Huffman, J. V. Snelling, T. E. Zipperian, A. J. Ricco, and C. A. Kelsey. (1988). "Miniature Radiation Dosimeter for *In Vivo* Radiation Measurements." *Int. J. Radiat. Oncol. Biol. Phys.* 14:963–67.

International Commission on Radiation Units and Measurement. *Quantities and Units in Radiation Protection Dosimetry.* ICRU Report 51. Bethesda, MD: ICRU, 1993.

Jursinic, P. A. (2007) "Characterization of Optically Stimulated Luminescence Dosimeters, OSLDs, for Clinical Dosimetric Measurements." *Med. Phys.* 34:4594–604.

Kerns, J. R., S. F. Kry, and N. Sahoo. (2012). "Characteristics of Optically Stimulated Luminescence Dosimeters in the Spread-out Bragg Peak Region of Clinical Proton Beams." *Med. Phys.* 39:1854–63.

Kirby, T. H., W. F. Hanson, R. J. Gastorf, C. H. Chu, and R. J. Shalek. (1986). "Mailable TLD System for Photon and Electron Therapy Beams." *Int. J. Radiat. Oncol. Biol. Phys.* 12:261–65.

Klassen, N. V., L. van der Zwan, and J. Cygler. (1997). "GafChromic MD-55: Investigated as a Precision Dosimeter." *Med. Phys.* 24:1924–34.

Kohno, R., K. Hotta, T. Matsuura, K. Matsubara, S. Nishioka, T. Nishio, M. Kawashima, and T. Ogino. (2011). "Proton Dose Distribution Neasurements Using a MOSFET Detector with a Simple Dose-weighted Correction Method for LET Effects." *J. Appl. Clin. Med. Phys.* 12:3431.

Kohno, R., K. Hotta, K. Matsubara, S. Nishioka, T. Matsuura, and M. Kawashima. (2012). "*In Vivo* Proton Dosimetry Using a MOSFET Detector in an Anthropomorphic Phantom with Tissue Inhomogeneity." *J. App. Clin. Med. Phys.* 13:3431.

Kry, S. F., P. Alavarez, A. Molineau, C. Amador, J. Galvin, and D. S. Followill. (2013). "Algorithms Used in Heterogeneous Dose Calculations Show Systematic Differences as Measured with the Radiological Physics Center's Anthropomorphic Thorax Phantom Used for RTOG Credentialing." *Int. J. Rad. Oncol. Biol. Phys.* 85:e95–100.

Lee, K. Y., K. K. L. Fung, and C. S. Kwok. (2005). "Dual-peak Dose Measurements for Radiochromic Films by a Newly Developed Spectral Microdensitometer." *Med. Phys.* 32:1485–90.

Lindsay, P., A. Rink, M. Ruschin, and D. Jaffray. (2010). "Investigation of Energy Dependence of EBT and EBT-2 Gafchromic Film." *Med. Phys.* 37:571–76.

Mack, A., S. G. Scheib, J. Major, S. Gianolini, G. Pazmandi, H. Feist, H. Czempiel, and H. Kreiner. (2002). "Precision Dosimetry for Narrow Photon Beams Used in Radiosurgery – Determination of Gamma Knife Output Factors." *Med. Phys.* 29:2080–89.

Mart, C. J., H. R. Elson, and M. A. Lamba. (2012). "Measurement of Low-energy Backscatter Factors Using GAFCHROMIC Film and OSLDs." *J. Appl. Clin. Med. Phys.* 13:3832.

Mayer, R. R., F. Ma, Y. Chen, R. I. Miller, A. Belard, J. McDonough, and J. J. O'Connell. (2012). "Enhanced Dosimetry Procedures and Assessment for EBT2 Radiochromic Film." *Med. Phys.* 39:2147–55.

McLaughlin, W. L., J. C. Humphreys, D. Hocken, and W. J. Chappas. (1988). "Radiochromic Dosimetry for Validation and Commissioning of Industrial Radiation Processes" in *Progress in Radiation Processing, Proceedings of the Sixth International Meeting*, F. M. Fraser, ed. *Radiat. Phys. Chem.* 31:505–514.

McLaughlin, W. L., Y. D. Chen, C. G. Soares, A. Miller, G. Van Dyke, and D. F. Lewis. (1991). "Sensitometry of the Response of a New Radiochromic Film Dosimeter to Gamma Radiation and Electron Beams." *Nucl. Instrum. Methods. Phys. Res. A* 302:165–176.

Mutscheller, A. (1928). "Safety Standards of Protection Against X-ray Dangers." *Radiology* 10:468.

Niroomand-Rad, A., C. R. Blackwell, B. M. Coursey, K. P. Gall, J. M. Galvin, W. L. McLaughlin, A. S. Meigooni, R. Nath, J. E. Rodgers, and C. Soares. (1998). "Radiochromic Film Dosimetry: Recommendations of AAPM Radiation Therapy Committee Task Group 55." *Med. Phys.* 25:2093–2115.

Nose, T., M. Koizumi, K. Yoshida, K. Nishiyama, J. Sasaki, T. Ohnishi, T. Kozuka, K. Gomi, M. Oguchi, I. Sumida, Y. Takahashi, A. Ito, and T. Yamashita. (2008). "*In Vivo* Dosimetry of High-Dose-Rate Interstitial Brachytherapy in the Pelvic Region: Use of a Radiophotoluminescence Glass Dosimeter for Measurement of 1004 Points in 66 Patients with Pelvic Malignancy." *Int. J. Radiat. Oncol. Biol. Phys.* 70:626–33.

Onal, C., A. Sonmez, G. Arslan, S. Sonmez, E. Efe, and E. Oymak. (2012). "Evaluation of Field-in-Field Technique for Total Body Irradiation." *Int. J. Radiat. Oncol. Biol. Phys.* 83:1641–48.

Ong, C. L., W. F. A. R. Verbakel, M. Dahele, J. P. Cuijpers, B. J. Slotman, and S. Senan. (2012). "Fast Arc Delivery for Stereotactic Body Radiotherapy for Vertebral and Lung Tumors." *Int. J. Rad. Oncol. Biol. Phys.* 83: e137–43.

Onori, S., F. d'Errico, C. De Angeles, E. Egger, P. Fattibene, and I. Janovsky. (1997). "Alanine Dosimetry of Proton Therapy Beams." *Med. Phys.* 24:447–53.

Perks, J., M. Gao, V. Smith, S. Skubic, and S. Goetsch. (2005). "Glass Rod Detectors for Small Field, Stereotactic Radiosurgery Dosimetric Audit." *Med. Phys.* 32:726–32.

Quinn, A., L. Holloway, E. Koh, G. H. Delaney, S. Arumugam, G. Goozee, and P. Metcalfe. (2012). "Radiation Dose and Contralateral Breast Cancer Associated with Megavoltage Cone-beam Computed Tomographic Image Verification in Breast Radiation Therapy." *Prac. Rad. Oncol.* 3:93–100.

Rah, J., D. H. Oh, J. W. Kim, D. Kim, T. Suh, Y. H. Ji, D. Shin, S. B. Lee, D. Y. Kim, and S. Y. Park. (2012). "Feasibility Study of Glass Dosimeter for *In Vivo* Measurement: Dosimetric Characterization and Clinical Application in Proton Beams." *Int. J. Radiat. Oncol. Biol. Phys.* 84:e251–56.

Scarantino, C. W., B. R. Prestidge, M. S. Anscher, C. R. Ferree, W. T. Kearns, R. D. Black, N. G. Bolick, and G. P. Beyer. (2008). "The Observed Variance between Predicted and Measured Radiation Dose in Breast and Prostate Patients Utilizing an *In Vivo* Dosimeter." *Int. J. Radiat. Oncol. Biol. Phys.* 72:597–604.

Scarantino, C. W., C. J. Rini, M. Aquino, T. B. Carrea, R. D. Ornitz, M. S. Anscher, and R. D. Black. (2005). "Initial Clinical Results of an *In Vivo* Dosimeter during External Beam Radiation Therapy." *Int. J. Radiat. Oncol. Biol. Phys.* 62:606–13.

Soubra, M., J. Cygler, and G. Mackay. (1994). "Evaluation of a Dual Bias Metal Oxide-Silicon Semiconductor Field Effect Transistor Detector as Radiation Dosimeter." *Med. Phys.* 21:567–72.

Smathers, J. B., V. A. Otte, A. R. Smith, P. R. Almond, F. H. Attix, J. J. Spokas, W. M. Quam, and L. J. Goodman. (1977). "Composition of A-150 Tissue-equivalent Plastic." *Med. Phys.* 4:74–77.

Thomsen, K. J. (2004.) "Optically Stimulated Luminescence Techniques in Retrospective Dosimetry Using Single Grains of Quartz Extracted from Unheated Materials." Risø National Laboratory. Risø-PhD; No. 1(EN).

Tien, C. J., R. Ebeling III, J. R. Hiatt, B. Curran, and E. Sternick. (2012). "Optically Stimulated Luminescent Dosimetry for High Dose Rate Brachytherapy." *Front. Oncol.* 2:91.

Wielopolski, L., M. Maryanski, B. Ciesielski, A. Forman, L.E. Reinstein, and A. G. Meek. (1987). "Continuous Three-dimensional Radiation Dosimetry in Tissue-equivalent Phantoms Using Electron Paramagnetic Resonance in L-α-alanine." *Med. Phys.* 14:646–52.